SAND REPORT

SAND2002-1014
Unlimited Release
Printed May 2002

Coupled Eulerian-Lagrangian Methods for Earth Penetrating Weapon Applications

Kevin H. Brown, Shawn P. Burns Mark A. Christon

Prepared by
Sandia National Laboratories
Albuquerque, New Mexico 87185 and Livermore, California 94550

Sandia is a multiprogram laboratory operated by Sandia Corporation, a Lockheed Martin Company, for the United States Department of Energy under Contract DE-AC04-94AL85000.

Issued by Sandia National Laboratories, operated for the United States Department of Energy by Sandia Corporation.

Available to DOE and DOE contractors from
U.S. Department of Energy
Office of Scientific and Technical Information
P.O. Box 62
Oak Ridge, TN 37831

Telephone: (865)576-8401
Facsimile: (865)576-5728
E-Mail: reports@adonis.osti.gov
Online ordering: http://www.doe.gov/bridge

Available to the public from
U.S. Department of Commerce
National Technical Information Service
5285 Port Royal Rd
Springfield, VA 22161

Telephone: (800)553-6847
Facsimile: (703)605-6900
E-Mail: orders@ntis.fedworld.gov
Online order: http://www.ntis.gov/ordering.htm

SAND2002-1014
Unlimited Release
Printed May 2002

Coupled Eulerian-Lagrangian Methods for Earth Penetrating Weapon Applications

Kevin H. Brown, Shawn P. Burns and Mark A. Christon
Computational Physics R&D Department
Sandia National Laboratories
P. O. Box 5800
Albuquerque, NM 87185-0819

Abstract

This report provides a review of the open literature relating to numerical methods for simulating deep penetration events. The objective of this review is to provide recommendations for future development of the ALEGRA shock physics code to support earth penetrating weapon applications. While this report focuses on coupled Eulerian-Lagrangian methods, a number of complementary methods are also discussed which warrant further investigation. Several recommendations are made for development activities within ALEGRA to support earth penetrating weapon applications in the short, intermediate, and long term.

Acknowledgements

The authors would like to thank Courtenay Vaughan, Ray Bell, and Greg Bessette for their description of the ZAPOTEC algorithm. The authors would also like to thank Sam Key for providing background information on the DYTRAN and PISCES codes.

Table of Contents

List of Figures

Executive Summary

The following report provides an assessment of the open literature regarding numerical simulation methods applicable to earth penetrating weapon (EPW) applications. Although, for completeness, a number of methods for deep penetration are discussed, the primary focus of this report is on coupled Eulerian-Lagrangian methods. Three main recommendations are made corresponding to the immediate, intermediate, and long term:

1) The SHISM arbitrary Lagrangian-Eulerian method (Budge, 1995) currently implemented within ALEGRA should be enhanced to relax the requirement for node-to-node mesh continuity. This may be accomplished using the contact capability provided by the ACME package (Brown, et al., 2001). Some additional work is also needed to more accurately compute the interaction force between the penetrator and the target interface of the Lagrangian and Eulerian (arbitrary Lagrangian-Eulerian) mesh.

2) The ZAPOTEC method (Attaway, et al., 2001) should be implemented within ALEGRA during the current fiscal year to provide a complimentary simulation capability that provides additional flexibility over that provided by SHISM. The fidelity of the ZAPOTEC method as well as the operational experience available within Sandia National Laboratories (Vaughan, Bessette, Bell, 2001) make this method an ideal choice for the intermediate term.

3) A vigorous research program focusing on other promising simulation techniques identified in this report should be supported for the long term. Research of this sort will be necessary to provide simulation flexibility and fidelity for future EPW development efforts.

Nomenclature

Underline	Vector
^	Unit vector
d	Displacement vector
F	Force vector
m	Mass
t	Time
V	Volume

Greek

ϕ	Volume fraction

Subscripts

E	Eulerian quantity
L	Lagrangian quantity

Acronyms

ALE	Arbitrary Lagrangian-Eulerian
CEL	Coupled Eulerian-Lagrangian
EPW	Earth Penetrating Weapon

1. Introduction

What are the most promising algorithms to support numerical simulation of Earth Penetrating Weapon (EPW) applications at Sandia? A partial response to this question can be obtained from a review of the open literature in numerical simulation of deep penetration and fluid-solid interaction. The citations reviewed in this report allow several recommendations to be made regarding some of the more promising methods for EPW simulations. The objective of this report is to provide a basis for future algorithm development of the ALEGRA[1] application within the NEVADA framework. The results of this literature review will help to guide the development of EPW application support within ALEGRA.

The following sections provide a high level overview of the different classes of shock physics simulation methodologies described in the open literature in the context of the EPW application of interest. This discussion will provide the background for the description of several representative deep penetration numerical simulation methodologies discussed in the next chapter. Finally, this report concludes by describing a strategy for developing a usable EPW simulation capability within ALEGRA over the next one to two years.

1.1 Earth Penetrating Weapon Application

The class of EPW applications of interest in this report consists of a deformable penetrator impacting either a semi-infinite or finite thickness target. The penetrator will undergo large displacement and can experience either moderate or large local deformation. The target, on the other hand, will undergo extreme deformations. The flexibility of the penetrator will influence the trajectory of the penetrator within the target and intimate contact between the penetrator and the target cannot be assumed as voids may open in the target material. Furthermore, the target material cannot be assumed to be homogeneous. Rock, rubble, voids, and man made structures may form part of the target. The penetrator, on the other hand, represents a complex collection of various manufactured materials including ductile metals, ceramics, and foams. Shell like members and fine detail will typically make up the penetrator design.

The performance metrics of interest for numerical simulation of EPW applications include reproduction of the overall trajectory of the weapon in the target including depth of penetration and the axial and lateral deceleration of the weapon. The structural response of the weapon as well as the acceleration environment of individual components within the weapon must also be reproduced. In addition to the weapon itself, the motion of the target material may also be of importance in evaluating weapon effects and fuzing. The precision and accuracy required will depend on the objectives of the numerical simulation being conducted.

1. An arbitrary Lagrangian-Eulerian multi-material finite element code that emphasizes large deformations and strong shock physics developed at Sandia National Laboratories.

1.2 Shock Physics Simulation Methodologies

Mair (1999), Benson (1992) and Anderson (1987) provide general descriptions of shock physics simulation methods over the last 15 years. Mair focuses on underwater explosion applications while Benson and Anderson provide more general descriptions of shock physics simulation[2] technology. Of particular interest here are the discussions by Benson and Anderson on general coupled Eulerian-Lagrangian formulations and pure Lagrangian simulation of deep penetration respectively. The following sections reflect the framework provided by these earlier reviews and discuss some of the advantages and disadvantages of various methodologies in the context of EPW applications.

1.2.1 Lagrangian Formulation

The principal advantage of a purely Lagrangian formulation is that the interface between the penetrator and target is precisely defined and tracked. Unfortunately, large deformations within the target region will lead to hopeless mesh tangling in a purely Lagrangian reference frame. Various approaches have been used to resolve the mesh tangling problem including rezoning and slideline algorithms in conjunction with element failure models to delete elements (Anderson, 1987). The principal drawback of the latter approach is the need to develop a physically realistic element failure model. Rezoning on the other hand can be successfully applied to impact problems but may be computationally expensive. Perforation of finite thickness targets also involves particular challenges with this approach[3]. Continued research into target rezoning is certainly warranted and is being conducted at Sandia (Jung, 2001).

1.2.2 Eulerian Formulation

An Eulerian reference frame avoids the difficulty of mesh tangling in the target but also looses the precise interface description provided by the Lagrangian formulation. Treating computational cells at the target-penetrator interface as mixtures of the target and penetrator material tends to dilute the material properties. This may result is excessive erosion of the penetrator material in a soft target (Siling, 1993). This problem must be handled by the introduction of a boundary layer model for cells at the target-penetrator interface. Another limitation in the use of purely Eulerian formulations in EPW applications is the representation of small features. Extremely fine zoning is required to avoid smearing out small features in an Eulerian EPW simulation (Mair, 1999) which could result in prohibitive mesh size and computation time.

---

2. Mair (1999) points out that the term “hydrocode” is misnomer as these codes are commonly used to simulate more than simply hydrodynamic behavior. We will use the term “shock physics simulation” in this report to imply that material strength may also be important.
3. An element death approach may be necessary to open up an exit surface on the back side of a finite thickness target.

1.2.3 Coupled Eulerian-Lagrangian Formulation

The coupled Eulerian-Lagrangian (CEL) method attempts to capture the strengths of the Lagrangian and Eulerian methods discussed above. In general, a Lagrangian reference frame is used to discretize the penetrator while an Eulerian frame is used to discretize the target. The boundary of the Lagrangian domain is typically taken to represent the actual interface between the penetrator and the target. Typical interface models use the velocity of the Lagrangian boundary as a kinematic constraint in the Eulerian calculation and the stress within the Eulerian cell to calculate the resulting surface force on the Lagrangian domain (Benson, 1992). Different CEL algorithms may be characterized by the details of how this interface condition is treated. CEL algorithms provide some of the most promising approaches to providing a usable, general purpose EPW simulation capability and will be the focus of this report. The specifics of several CEL algorithms will be described later in this report.

1.2.4 Arbitrary Lagrangian-Eulerian Formulation

Arbitrary Lagrangian-Eulerian (ALE) formulations are commonly discussed in the fluid structure interaction literature. For example, Belytschko, et al. (1982) and Donea, et al. (1982), describe the use of ALE methods in nuclear safety calculations. ALE methods provide for the arbitrary motion of the computational mesh and provide a means of developing a continuous mesh between a fixed (Eulerian) target and the deforming (Lagrangian) penetrator. As a result, the target-penetrator interface is internal to the discretization and many of the heuristics employed by CEL methods can be removed or simplified.

The large displacement experienced by the penetrator in EPW applications can still result in mesh tangling in ALE methods. One approach suggested by Budge (1995) to handle the large displacement problem is to run in a reverse ballistic mode where the target material moves rather than the penetrator. While a reverse ballistic approach has been adopted in the SHISM algorithm (Budge, 1995), additional development will be needed to handle multiple penetrators as well as inflow boundary conditions to model semi-infinite targets.

1.2.5 Meshfree Methods

Meshfree methods may be considered particular types of Lagrangian methods (Mair, 1999) but they are discussed separately here due to their unique characteristics. Mesh free methods such as smooth particle hydrodynamics (Wingate, Stellingwerf 1993) avoid the problem of mesh tangling in the target since they do not employ explicit nodal connectivity. Thus, nodes are allowed to move about the domain in a Lagrangian fashion and interactions between nodes are determined as part of the computation. This determination of nodal interactions without an explicit mesh tend to make meshfree methods computationally expensive. Nevertheless, coupling of meshfree target representations with traditional Lagrangian penetrator representations have been discussed by Attaway, et al. (1993) and Silling (2001) and research into these methods is continuing at Sandia.

1.3 Scope

The discussion presented above gives some indication of the variety of numerical methods that have been applied to deep penetration problems. For the purpose of this report, both pure Lagrangian and pure Eulerian methods are considered to be too limited for further consideration. ALE methods, while having some advantages over purely Lagrangian and Eulerian methods, have significant limitations when dealing with the large displacements that characterize EPW applications. Meshfree methods, on the other hand, may offer a method for overcoming the mesh tangling problem experienced by Lagrangian and ALE methods. Modification would be required in the ALEGRA framework to support a meshfree structure. While this is certainly possible within the next one to two years, the CEL methods seem to be a better choice at this time. We will return to both ALE and meshfree methods later in the recommendations section of this report.

The remainder of this report will focus on CEL algorithms as being the most promising method for developing a usable EPW simulation capability within the ALEGRA program in the one to two year time frame. The next chapter will focus on the details of several CEL algorithms which represent fruitful approaches taken in the past. The discussion presented in this introduction as well as in the next chapter are used to support the final recommendations.

2. Coupled Eulerian-Lagrangian Methods

The following sections describe in some detail three coupled Eulerian-Lagrangian (CEL) methods which are thought to be representative of the successful approaches taken in the past to numerical simulation of deep penetration. The methods described here are representative of the methods implemented in the DYTRAN nonlinear transient dynamics code[1], the LS-DYNA large deformation structural response code[2] (Hallquist, 1998), and the ZAPOTEC code[3] (Attaway, et al. 2001). In addition to these methods, several other promising technological approaches are described in the last section of this chapter.

2.1 Noh's Method

Although somewhat dated, the method described by Noh (1964) represents the original coupled Eulerian-Lagrangian method and predates other CEL literature. This method also provided the basis for the algorithm employed in the PISCES 2DELK code (Hancock, 1985). Noh's method is described here because it represents a fairly intuitive approach to the coupling between the Eulerian and Lagrangian domains. While Noh's original work was in two spatial dimensions, the extension to three dimensions is conceivable although the implementation is not particularly straight forward.

Noh's method (Noh, 1964) is shown schematically in Figure 1. Assume that at some time, t^n, the position of the Lagrangian domain is known and the state of all materials is known, e.g., density, pressure, etc. Also, assume that the subset of the Eulerian domain which is interior to, on the boundary of, and external to the Lagrangian domain at t^n is known. The method described by Noh proceeds in three distinct phases to obtain the solution at the next time step t^{n+1}. During the first phase, the motion of the Lagrangian domain is calculated using the current pressures in the Eulerian material to calculate the forces acting on the surface of the Lagrangian domain. Several Lagrangian steps can be taken for each Eulerian calculation (subcycling). In the second phase, the portion of the Eulerian domain outside the Lagrangian domain is determined using the new position of the Lagrangian domain. Discrete equations must be developed for the irregularly shaped Eulerian cells that make up the interface between the Eulerian and Lagrangian domains. Finally, the descretized Eulerian equations are solved to obtain the new pressures that will act on the Lagrangian domain during the next time step.

The discrete Eulerian equations are derived using Green's theorem[4] to form the discrete conservation equation for the control volume around each Eulerian node as shown in Figure 1. The same approach is used for the arbitrary polygonal cells which form the interface with the Lagrangian domain. For interface cells, the velocity of the Eulerian material at cell boundaries corresponding to the Lagrangian boundary is set equal to the

1. Marketed by MSC Software, Los Angeles, CA
2. Marketed by Livermore Software Technology Corporation, Livermore, CA
3. Developed at Sandia National Laboratories, Albuquerque, NM
4. Green's Theorem: $\iint_A \left(\frac{\partial N}{\partial x} - \frac{\partial M}{\partial y}\right) dx dy = \oint_{\partial A} (M dx + N dy)$

velocity of the Lagrangian boundary. Small Eulerian cells are also combined with neighboring cells to avoid time step limitations.

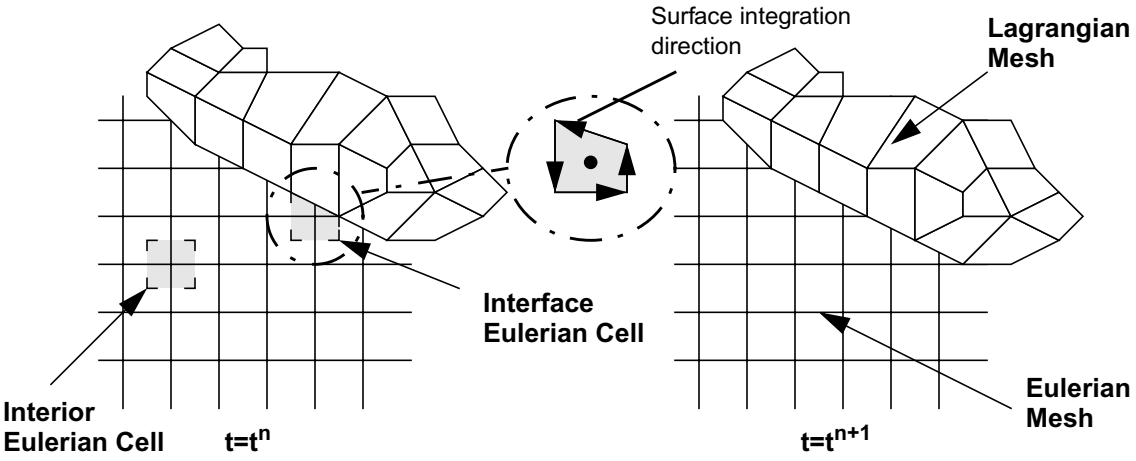

Figure 1 Noh's coupled Eulerian-Lagrangian method.

The development of the discrete Eulerian equations for interface cells is simplified in Noh's formulation (Noh, 1964) by assuming plane geometry and by using a structured Eulerian grid. While Noh's method can be extended to three dimensions using Gauss' divergence theorem[5], defining and calculating the necessary surface integrals would be considerably more cumbersome. Also, it is not clear that Noh's method accounts for inertial effects, i.e. added mass, when calculating the forces applied to the Lagrangian domain. The acceleration of the Eulerian material by the Lagrangian domain is not reflected by the pressure in the Eulerian cell. This added mass effect would act to increase the effective force acting on the Lagrangian domain (Panton, 1984).

2.2 The Penalty Method

Noh's method employed a coupling between the Lagrangian and Eulerian domains similar to that described by Benson (1992). That is, the velocity of the Lagrangian boundary provides a kinematic constraint on the Eulerian calculation and the pressures in the Eulerian material provides forces on the Lagrangian domain. An alternative coupling is described by Olovsson (2000) that shares many similarities with general contact algorithms.

Olovsson's method (Olovsson, 2000) is shown schematically in Figure 2. At the beginning of the time step t^n, the location of any Lagrangian node that lies within each Eulerian cell is noted. Using the interface forces calculated in the previous time step, the motion of *both* the Lagrangian domain and the Eulerian material are calculated. The relative displacement between the Eulerian material point and the Lagrangian node is calculated at the end of the time step and a penalty force is applied to both the Lagrangian and Eulerian nodes.

5. Gauss Divergence Theorem: $\iiint_V (\nabla \bullet \underline{F}) dV = \int\int_{\partial V} \underline{F} \bullet \hat{n} dA$

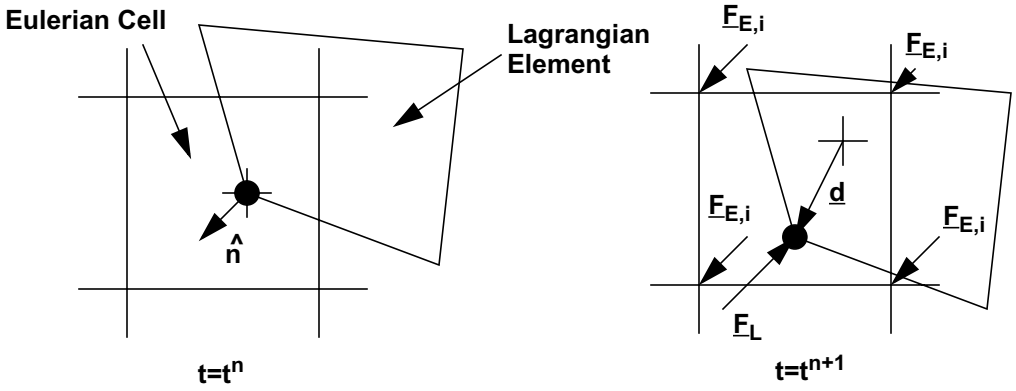

Figure 2 Olovsson's penalty method for coupled Eulerian-Lagrangian domains.

The forces applied at the Eulerian and Lagrangian nodes are calculated from the penalty force, $\underline{F}_p$

$$\underline{F}_p = k_p \underline{d}_p, \tag{1}$$

where k_p is the penalty stiffness (to be defined shortly), and $\underline{d}_p$ is the penalty displacement. The penalty displacement in Equation (1) is calculated from the normal and tangential components of the relative displacement vector

$$\underline{d}_n = (\underline{d} \bullet \hat{n})\hat{n}, \tag{2}$$

$$\underline{d}_t = \underline{d} - \underline{d}_n, \tag{3}$$

where $\underline{d}$ is the actual displacement as shown in Figure 2 and $\hat{n}$ is the outward directed normal vector to the Lagrangian surface at the Lagrangian node. The penalty force is applied only if the relative motion of the Eulerian material point and the Lagrangian node is compressive, i.e.,

$$\underline{d} \bullet \underline{n} > 0. \tag{4}$$

Olovsson (2000) uses the interface friction to calculate the penalty displacement shown in Equation (1)

$$\underline{d}_p = \begin{cases} \underline{d}_n & \text{if } \mu_f = 0 \\ \underline{d}_n + \mu_f \dfrac{|\underline{d}_t|}{|\underline{d}_n|}\underline{d}_t & \text{if } |\underline{d}_n| < \mu_f |\underline{d}_t| \\ \underline{d} & \text{if } |\underline{d}_n| \geq \mu_f |\underline{d}_t| \end{cases}, \tag{5}$$

where μ_f is the coefficient of friction.

The penalty stiffness shown in Equation (1) is simply the inertial stiffness

$$k_p = \varepsilon \frac{\tilde{m}}{\Delta t^2}, \tag{6}$$

where Δt is the time step size and $\tilde{m}$ is the minimum of the Lagrangian and Eulerian mass

$$\tilde{m} = min\{m_L, m_E\}. \tag{7}$$

The Eulerian mass, m_E, is calculated by using the Eulerian cell basis functions to map the nodal mass values to the location of the Lagrangian node at the *end* of the time step. The Lagrangian mass, m_L, is simply the mass of the Lagrangian node. The penalty force in essence adds a new spring-mass system to the problem. To avoid time step limitations, the penalty stiffness includes a small multiplier, ε, as shown in Equation (6). This multiplier makes the natural frequency of the spring mass system represented by the penalty force much lower than that of the overall problem (Hallquist, 1998). Hallquist suggests a value of 4% for the contact algorithm in LS-DYNA while Olovsson (2000) suggests a value of 5%.

Once the penalty stiffness and displacement are calculated, the penalty force may then be calculated from Equation (1). The resulting forces applied to the Eulerian nodes are determined using the Eulerian cell basis functions

$$\underline{F}_{E,i} = N_i \beta_i \underline{F}_p, \tag{8}$$

where $\underline{F}_{E,i}$ is the force applied at node i of the Eulerian cell and N_i is the ith Eulerian basis function evaluated at the location of the Lagrangian node at the *end* of the time step. The weight function scales the Eulerian nodal force depending on the Eulerian mass at each node, $m_{E,i}$,

$$\beta_i = min\left\{1, \frac{m_{E,i}}{(N_i + 0.001)\tilde{m}}\right\}. \tag{9}$$

So, the force applied to an Eulerian node will go to zero as the mass at that node goes to zero. The force applied to the Lagrangian node is simply equal and opposite to the sum of the Eulerian forces

$$\underline{F}_L = -\sum_i \underline{F}_{E,i}. \tag{10}$$

The forces applied to the Eulerian and Lagrangian nodes in Olovsson's method (Olovsson, 2000) will tend to push the Eulerian material away from the Lagrangian surface. Olovsson's method does not rigorously enforce no interpenetration of the Eulerian material into the Lagrangian domain. Indeed, if the Eulerian mesh spacing is much less than that of the Lagrangian mesh then Eulerian material can "leak" past the Lagrangian surface. This is because, for fine Eulerian mesh spacing, there will be Eulerian cells that do not contain a Lagrangian node and therefore do not receive any restoring force. One

can imagine various ways to relieve this problem, for example, by using Lagrangian integration point locations rather than nodal locations. The same mass leakage problem will not occur if the Lagrangian mesh spacing is much less than that of the Eulerian mesh.

2.3 The ZAPOTEC Method

The methods described by Noh (1964) and Olovsson (2000) employed explicit velocity or force boundary conditions to represent the motion of the Lagrangian domain in the Eulerian calculation. In contrast, the ZAPOTEC method (Vaughan, Bessette, Bell, 2001, Attaway, et al. 2001) maps the Lagrangian material directly into the Eulerian calculation at each timestep. Eulerian cells inherit the Lagrangian material state, i.e., density, pressure, etc., from the Lagrangian domain prior to taking the next Eulerian time step. In this way, the effect of the Lagrangian motion on the Eulerian material is implicitly calculated rather than explicitly calculated as in the case of the methods described by Noh and Olovsson. It is still necessary, however, to calculate the forces acting on the Lagrangian domain due to the Eulerian material motion.

The ZAPOTEC method is described schematically in Figure 3. At the start of time step t^n, the position of the Lagrangian domain is known and the state of all Lagrangian and Eulerian materials are known. The first step in the ZAPOTEC method is to calculate the overlap volume between each element in the Lagrangian domain and any Eulerian cells intersected by that element. Once this is done, the volume fraction of the Lagrangian material within each Eulerian cell is known. The volume fraction of the Eulerian material within the same cell is known from the previous Eulerian time step.

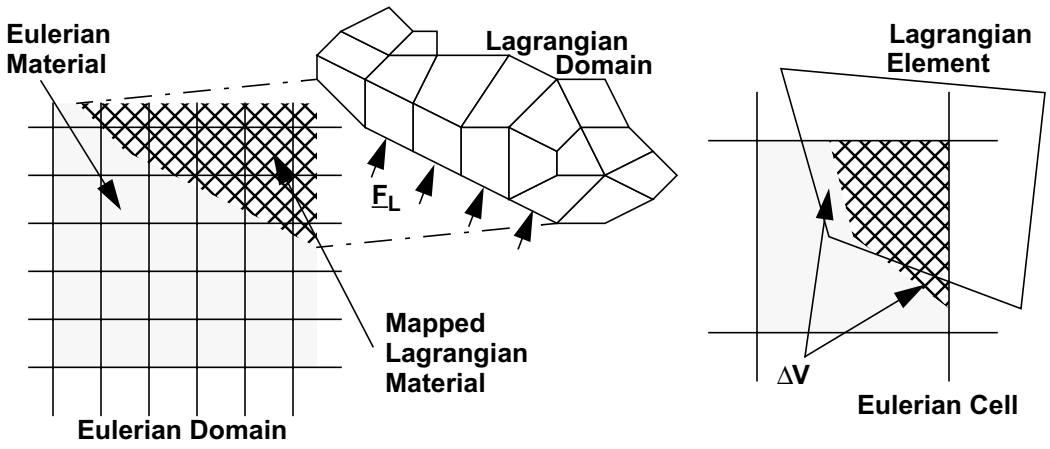

Figure 3 The ZAPOTEC coupled Eulerian-Lagrangian method.

Ideally, the volumes of the Lagrangian and Eulerian materials should sum to be the same as the volume of the cell. As will become clear, this will not necessarily be the case since the motion of the Lagrangian domain is calculated independently from the Eulerian calculation, it is close however. The resulting volume difference

$$\Delta V = V_{cell} - \sum_i V_i, \tag{11}$$

where the subscript i indicates each material in the cell (Lagrangian or Eulerian), must be allocated between the Eulerian and Lagrangian materials. Vaughan, et al. (2001) describe a distribution scheme based on a weighting parameter, ϕ_i, for each material in the cell

$$\phi_i = \frac{V_i^2/\rho_i}{\sum_j V_j^2/\rho_j}. \tag{12}$$

The corrected volume for each material in an overfilled cell, i.e. $\Delta V<0$, is then given by

$$\tilde{V}_i = V_i + \frac{\phi_i}{\sum_j \phi_j}\Delta V \tag{13}$$

where the ~ indicates the corrected volume for each material in the cell. The volume correction is only performed for overfilled cells, not for cells with partial void volume, i.e. $\Delta V>0$. Equation (12) and Equation (13) will tend to allocate any volume change resulting from Equation (11) to the material with the lowest density while neglecting materials with very small volume.

Once the correct volume fractions are known, the Lagrangian material is mapped into the Eulerian cell and that cell inherits the Lagrangian material density, pressure, internal energy[6], etc. The pressure within the Eulerian cell is then calculated from the volume averaged pressure of all Eulerian and Lagrangian materials within it. The individual material pressures may also be augmented by any additional compression of the materials resulting from Equation (12) and Equation (13). All other cell properties are mass averages of the individual material properties.

At this point, the next Lagrangian and Eulerian time steps are taken independently. The forces acting on the Lagrangian domain for the next time step are calculated from the stress state in the neighboring Eulerian cells. The Eulerian calculation carries the mapped Lagrangian material through the next Eulerian time step calculation. As discussed previously, the motion of the mapped Lagrangian material and the Lagrangian domain should correspond exactly ideally.

In the ZAPOTEC algorithm, the Lagrangian-to-Eulerian coupling is handled implicitly, including inertial effects, by the presence of the mapped Lagrangian material in the Eulerian calculation. The converse is not true however and must be accounted for by evaluating the force acting on the Lagrangian domain. Also, the procedure described above does not account for the effect of the added mass on the Lagrangian domain

6. The internal energy of the mapped Lagrangian material is only used when material donation, i.e., penetrator ablation, is being considered and Lagrangian material is permanently donated to the Eulerian calculation.

(Panton, 1984). Vaughan, Bessette, and Bell (2001) suggest that the method described above tends to overpredict the velocity of the Lagrangian domain[7]. It is possible that the added mass effect could account for part of this overprediction.

It is worth noting that one of the most expensive calculations in the ZAPOTEC method described above is the volume overlap calculation between the Lagrangian and Eulerian cells. A very precise calculation for the intersection of a tetrahedral with a hexahedral is used for this intersection calculation. Some computational savings might be obtained by using a less precise intersection between a tertrahedral and a right, rectangular solid or parallelpiped.

2.4 Other Methods

In addition to the CEL algorithms discussed above, several other promising approaches to the deep penetration problem can be found in the literature. These methods have many promising characteristics and should be considered as strong candidates for future development.

2.4.1 The SHISM Method

The SHISM method suggested by Budge (1995) employes an arbitrary Lagrangian-Eulerian formulation to avoid the difficulties of explicitly coupling Lagrangian and Eulerian domains. The ALE formulation permits a continuous computational mesh to be used between the Eulerian target domain and the Lagrangian penetrator. The interface models employed in the CEL methods discussed above become internal to the discretization and the interface mechanics is handled in a very natural way.

As discussed in the previous chapter, however, ALE methods cannot completely avoid mesh tangling problems in deep penetration applications. Budge (1995) resolves this difficulty by running in a reverse ballistic fashion as shown in Figure 4. By defining a reference velocity for the ALE region, the target can be thought of as moving past the penetrator. Any relative motion of the Lagrangian penetrator relative to the ALE region can be accommodated by the remap step in the ALE region. Additional flexibility can be obtained by including a rotational component in the reference velocity that corresponds to any gross rotation of the penetrator imparted by the target material[8].

While avoiding mesh tangling, the SHISM method does have a couple important limitations. A thick or semi-infinite target will require some kind of inflow boundary condition for the Eulerian domain. Such a condition may be difficult to implement for complex nonhomogeneous target or for a rotating Eulerian domain. The interaction of multiple penetrators with a single target would also be challenging using the SHISM method. Finally, although the contact calculation does account for some inertial effects,

7. Recent developments in ZAPOTEC may have resolved the velocity overprediction problem.
8. The rotational component is calculated by integration over the nodes of a specified set of element blocks in the Lagrangian penetrator.

improvements may be needed in the SHISM method to fully account for the effect of added mass (Panton, 1984) on the motion of the Lagrangian domain.

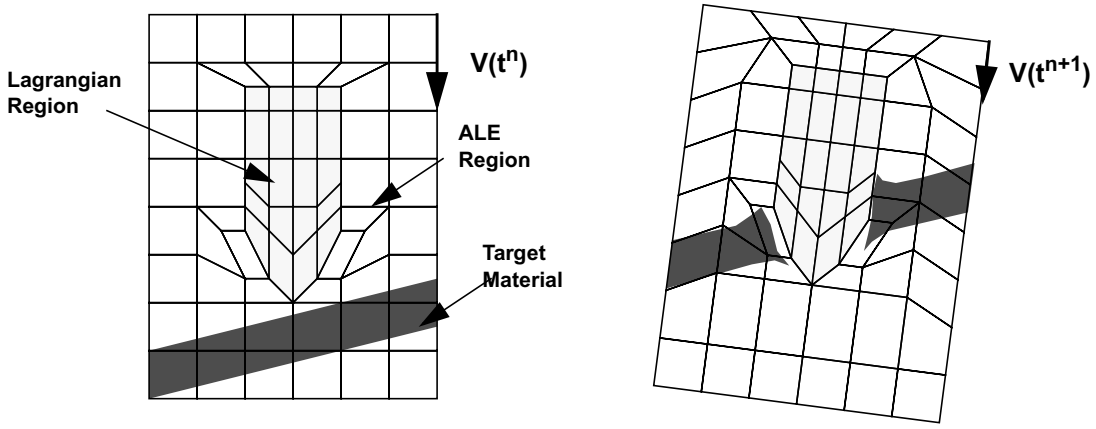

Figure 4 The SHISM arbitrary Lagrangian-Eulerian method.

Nevertheless, the ALE nature of the SHISM method is a natural fit to the ALEGRA architecture and has already been implemented. Improvements to the SHISM implementation can be made to relax the requirement of node-to-node mesh continuity between the ALE region and the Lagrangian region using the contact capability provided in the ACME package (Brown, et al., 2001). This improvement will simplify the mesh generation task significantly. Some additional work is also needed to more accurately compute the interaction force at the penetrator/target interface.

2.4.2 The Ghost Fluid Method

The ghost fluid method described by Fedkiw, et al. (1999) and applied to Eulerian-Lagrangian coupling by Arienti, et al. (2001) may also be a promising approach for earth penetrating weapon (EPW) applications. The ghost fluid method uses a level set to track the position on the Eulerian-Lagrangian interface at each time step as shown in Figure 5. The ghost fluid extended across the Eulerian-Lagrangian interface into the Lagrangian domain is based on the bulk properties of the Eulerian material. The state of the ghost fluid in the Lagrangian domain is based upon a thermodynamically consistent state that corresponds to the physical jump conditions at the interface. In this way, the ghost fluid velocities reflect the presence of both the Eulerian material and the Lagrangian interface in the solution method.

2.4.3 Smooth Particle Hydrodynamics Coupling

Swegle, et. al. (1993) describe a Lagrangian mesh free method that has been successfully used as a target region for EPW simulations (Metzinger, 1997). While this method has some very attractive features, it does suffer from a tensile instability which causes numerical fracture to occur. This fact coupled with the complexity of implementing this

technique in ALEGRA (primarily due to the parallel complexity) does not make this an attractive method for implementation in ALEGRA at this point.

2.4.4 Peridynamics Coupling

Silling (2001) describes a meshfree method for the target region based on peridynamic theory. In addition to the advantages of meshfree methods described in the previous chapter, Silling's formulation is also capable of simulating fracture and damage propagation. Brittle fracture is an important phenomena in EPW simulations involving geologic materials. With this method, the target space could be modeled as a Peridynamics region while the penetrator is modeled using a Lagrangian finite element region. The two regions would be coupled using a contact algorithm approach similar to what was done for Lagrangian finite element to SPH coupling as described by Swegle, et. al. (1993). Challenges remain in implementing a meshfree method in the ALEGRA architecture and further development will be required for a production capability. This method is more attractive than the SPH alternative due to the tensile instability in SPH and it would require less work to implement in ALEGRA due to different element requirements and a simpler parallel strategy.

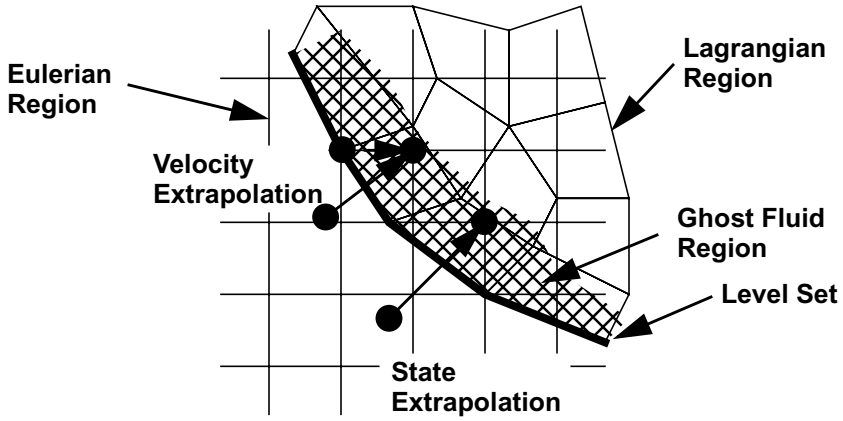

Figure 5 Ghost fluid method for coupled Eulerian-Lagrangian coupling.

2.4.5 Chimera Overset Grids

Chimera overset grids (Prewitt, et al., 2000) may provide a mechanism for overcoming some of the limitations of ALE methods such as the SHISM method described above (Budge, 1995). Rather than running in a reverse ballistic manner as described by Budge, an ALE region containing a Lagrangian penetrator might be overset on a Eulerian grid as shown in Figure 6. The ALE region could include both block structured and unstructured regions which may simplify mapping between inter-grid boundary points on the Eulerian background grid and the ALE grid. As in the SHISM method, the ALE grid could be given

a reference velocity and solid body rotation which corresponds to the center of gravity of the Lagrangian region to minimize mesh distortion.

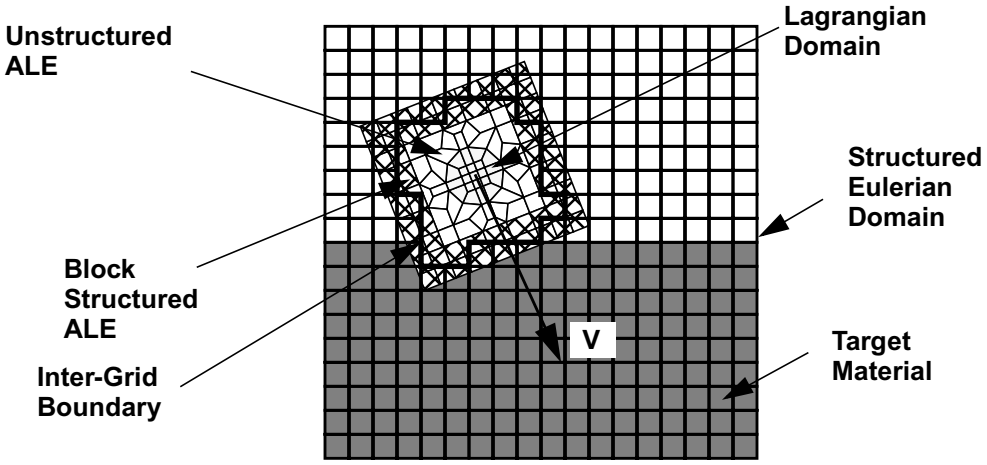

Figure 6 Chimera overset grids using arbitrary Lagrangian-Eulerian grids.

3. Recommendations

From the discussion presented in the previous chapters it is possible to make several recommendations regarding the development of a usable earth penetrating weapon (EPW) simulation capability within the ALEGRA architecture. The time frame of interest lies within the current fiscal year so the recommendations presented below are separated into three categories for immediate, current fiscal year, and out year efforts.

3.1 Immediate

The SHISM capability described by Budge (1995) has already been implemented in the ALEGRA framework and provides an interim simulation capability for a number of EPW applications. Improvements have already been made that employ the contact algorithms in ACME (Brown, et al., 2001) to relax the node-to-node connectivity requirements in the original SHISM implementation. One current deficiency in SHISM is the computation of the interaction force. This is currently being calculated by ACME which has an implicit assumption of Lagrangian materials. Better algorithms are currently being developed in ACME and will be available for SHISM in the short term. These new algorithms will provide a more accurate computation of the interaction force and therefore provide a higher fidelity solution. The SHISM capability will be validated against the experimental data provided by Forrestal et al., (1988).

3.2 Current Fiscal Year

Although all of the coupled Lagrangian-Eulerian (CEL) methods described in this report are derived from sound physical reasoning, the ZAPOTEC method (Vaughan, Bessette, Bell, 2001, Attaway, et al. 2001) enjoys some distinct advantages. By implanting the Lagrangian material to the Eulerian calculation, the ZAPOTEC method removes many of the more heuristic characteristics of other CEL methods. The ZAPOTEC method also maps onto the ALEGRA architecture well making its implementation easier, though certainly not effortless. Operational experience with the ZAPOTEC algorithm also exists within Sandia National Laboratories. This experience will be invaluable particularly when considering the parallel implementation of the ZAPOTEC method. Although computational efficiency issues are somewhat harder to assess, none of the other CEL methods considered in this study provide clear advantages over the ZAPOTEC method. Additionally, ZAPOTEC has been applied to EPW and shown to produce reasonable results. Current efforts at Sandia continue to improve the quality of the solutions. The success of the other methods when applied to EPW problems is less certain. For these reasons it is recommended that the ZAPOTEC method be adopted as the principal thrust of the ALEGRA EPW capability development effort for the current fiscal year.

3.3 Out Years

It is unlikely that a single method will provide an adequate modeling capability for all EPW simulation applications either in terms of speed or fidelity. Therefore a number of different modeling approaches should be pursued after an initial capability is established within ALEGRA. Several promising, if immature, methods have been discussed in this

report. Some of these methods are already being studied and developed for applications other that EPWs. The EPW modeling effort should remain connected with these other efforts while sponsoring research in a number of methods in the future. We believe that particular attention should be given to the Ghost Fluid Method and a coupling of the ALEGRA's solid dynamics for the penetrator with a Peridynamic region for the target space.

APPENDIX A

ZAPOTEC Volume Difference Limiting Cases

Consider a two material problem indicated by the subscripts E and L. Now consider the following cases:

Case 1 : $\rho_L \to 0$

By Equation (12) on page 22

$$\phi_E = \frac{\rho_L V_E^2}{\rho_L V_E^2 + \rho_E V_L^2} \to 0,$$

and by Equation (13) on page 22

$$\tilde{V}_E \to V_E.$$

Case 2: $\rho_E \to 0$

By Equation (12) on page 22

$$\phi_E = \frac{\rho_L V_E^2}{\rho_L V_E^2 + \rho_E V_L^2} \to 1,$$

and by Equation (13) on page 22

$$\tilde{V}_E \to V_E + \Delta V.$$

By Equation (11) on page 22 then

$$\tilde{V}_E \to V_E + V_{cell} - V_E - V_L = V_{cell} - V_L.$$

Case 3: $V_L \to 0$

By Equation (12) on page 22

$$\phi_E = \frac{\rho_L V_E^2}{\rho_L V_E^2 + \rho_E V_L^2} \to 1,$$

and, as above

$$\tilde{V}_E \to V_{cell} - V_L \to V_{cell}.$$

Case 4: $V_E \to 0$

By Equation (12) on page 22

$$\phi_E = \frac{\rho_L V_E^2}{\rho_L V_E^2 + \rho_E V_L^2} \to 0,$$

and, as above

$$\tilde{V}_E \to V_E.$$

APPENDIX B

ZAPOTEC Lagrangian Material Insertion Algorithm

The following procedure outlines the Lagrangian material insertion algorithm for each cell in the Eulerian mesh

Step 1 :

Determine the overlap of each Lagrangian element which intersects the Eulerian cell of interest, $\Delta V^L_{e(i)}$, where the superscript and subscript indicate a Lagrangian element of material i. The total volume of Lagrangian material i within the Eulerian cell is then

$$V_i^L = \sum_{e(i)} \Delta V^L{}_{e(i)}.$$

Step 2 :

Calculate the mass donated from each Lagrangian element to the Eulerian cell as the volume average of the mass in the element

$$\Delta m^L_{e(i)} = m^L_{e(i)} \frac{\Delta V^L_{e(i)}}{V^L_{e(i)}}.$$

The total mass of Lagrangian material i in the Eulerian cell is then

$$m_i^L = \sum_{e(i)} \Delta m^L{}_{e(i)}.$$

Step 3 :

Mass weight the donated momentum, internal energy, stress deviators, and sound speed from each Lagrangian cell. The donated internal energy, for example, is given by

$$\Delta E^L_{e(i)} = \frac{\Delta m^L_{e(i)} E^L_{e(i)}}{\sum_i m_i^L + \sum_j m_j^E},$$

So that the total donated internal energy from Lagrangian material i is

$$E_i^L = \sum_{e(i)} \Delta E^L{}_{e(i)}.$$

The half index shift algorithm (cf. APPENDIX A) is used to calculate the interface velocities using the total mass and momentum in the cell, including donated mass and momentum, during the next Eulerian time step.

Step 4 :

Volume weight the donated pressure from each Lagrangian element using the volume of the Lagrangian and Eulerian materials

$$\Delta P^L_{e(i)} = \frac{\Delta V^L_{e(i)} P^L_{e(i)}}{\sum_i V^L_i + \sum_j V^E_j}.$$

Notice that the total Eulerian cell volume is not used in calculating the donated pressure to account for Eulerian cells containing void (underfilled cells). The total pressure of Lagrangian material i is in the Eulerian cell is then

$$P^L_i = \sum_{e(i)} \Delta P^L{}_{e(i)}.$$

Step 5 :

Calculate the volume difference between the total cell volume and the sum of the Lagrangian and Eulerian material volumes

$$\Delta V = V_{cell} - \sum_i V^L_i - \sum_j V^E_j,$$ [1]

for overfilled cells, i.e. $\Delta V<0$, allocate the volume difference as described by Equation (12) and Equation (13) on page 22. Update the pressure of each material in the cell (Lagrangian and Eulerian) using the bulk modulus of the material

$$\tilde{P}_i = P_i - \rho_i C_i^2 \frac{\left|V_i - \tilde{V}_i\right|}{V_i},$$

where C is the sound speed, ρ is the density, $\tilde{P}_i$ is the updated pressure and $\tilde{V}_i$ is the updated material volume from Equation (13) on page 22. Update the internal energy of each material with the resulting flow work

$$\tilde{E}_i = E_i - \tilde{P}_i \left|V_i - \tilde{V}_i\right|.$$

1. This equation is the same as Equation (11) on page 22. In the latter case, the two summations have been combined into a single summation and the L and E superscripts indicating Lagrangian and Eulerian materials has been dropped for simplicity.

APPENDIX C

ZAPOTEC Half Index Shift Algorithm

Consider the one dimensional cell patch shown

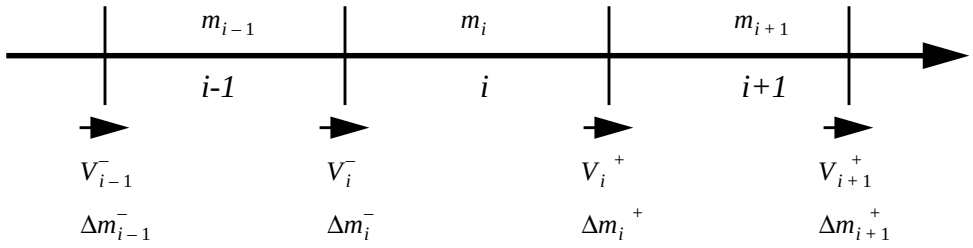

where m is the mass, V is the face velocity, Δm is the mass flux calculated at the end of the Lagrangian step, and i is the cell index number. The + and - superscripts indicate the faces of the cell as indicated. Note that the velocities carry the flow direction so that $V_i^+ < 0$ if the flow crossing the + face of cell i is in the -x direction for example. The mass flux across each face, on the other hand, is an absolute value so that $\Delta m_i^+ = \Delta m_{i+1}^-$.

The half index shift algorithm calculates the updated face velocities at the end of the Lagrangian step. The interface velocity at a given face is simply the ratio of the conservation of momentum and conservation of mass over the two cells which share the face. For example, for the + face of cell i

$$\tilde{V}_i^+ = \frac{V_i^+ (m_i + m_{i+1}) + V_i^- \Delta m_i^- - V_{i+1}^+ \Delta m_{i+1}^+}{m_i + m_{i+1} + \Delta m_i^- - \Delta m_{i+1}^+},$$

and similarly for the - face of cell i

$$\tilde{V}_i^- = \frac{V_i^- (m_i + m_{i-1}) + V_{i-1}^- \Delta m_{i-1}^- - V_i^+ \Delta m_i^+}{m_i + m_{i-1} + \Delta m_{i-1}^- - \Delta m_i^+}.$$

Similar equations may be constructed for two or three dimensional structured grids.

Bibliography

Anderson,C.E. 1987, "An Overview of the Theory of Hydrocodes," *International Journal of Impact Engineering*, 5(1-4):33-59

Arienti,M., Hung,P., Morano,E., .Shepherd,J.E, 2001, "A Level Set Approach to Eulerian-Lagrangian Coupling," *Journal of Computational Physics*, Submitted

Attaway, S.W., Heinstein, M.W., Mello, F.J., Swegle, J.W., 1993, "Coupling of Smooth Particle Hydrodynamics with Pronto," *Advances in Numerical Simulation Techniques for Penetration and Perforation of Solids, AMD-Vol.171*, E.P.Chen, V.K.Luk, ed., American Society of Mechanical Engineers, Applied Mechanics Division, pp. 83-94

Attaway, S.W., Bell, R.L., Vaughan, C.T., Goudy, S.P., Morrill, K.B., 2001, "Experiences with Coupled Codes for Modeling Explosive Blast Interacting with a Concrete Building," *Proceedings of the Workshop on Coupled Eulerian and Lagrangian Methodologies*, San Diego, CA, January, 22-24

Belytschko, T., Flanagan, D.P., Kennedy, J.M., 1982, "Finite Element Methods with User-Controlled Meshes for Fluid-Structure Interaction," *Computer Methods in Applied Mechanics and Engineering*, 33(1-3):669-688

Benson, D.J., 1992, "Computational Methods in Lagrangian and Eulerian Hydrocodes," *Computer Methods in Applied Mechanics and Engineering*, 99:235-394

Brown, K.H., Summers, R.H., Glass, M.W., Gullerud, A.S., Heinstein, M.W., Jones, R.E., 2001, "ACME Algorithms for Contact in a Multiphysics Environment, API Version 1.0," Technical Report SAND2001-3318, Sandia National Laboratories, Albuquerque, NM

Budge, K.G., 1995, "An Evaluation of Various Approaches to Simulating Hard/Soft Interactions," *Draft Technical Report*, Sandia National Laboratories, Albuquerque, NM

Donea, J., Giuliani, S., Halleux, J.P., 1982, "An Arbitrary Lagrangian-Eulerian Finite Element Method for Transient Dynamic Fluid-Structure Interactions," *Computer Methods in Applied Mechanics and Engineering*, 33(1-3):689-723

Fedkiw, R.P., Aslam, T., Merrimann, B., Osher, S., 1999, "A Non-Oscillatory Eulerian Approach to Interfaces in Multimaterial Flows (The Ghost Fluid Method)," *Journal of Computational Physics*, 152:457-492

Forrestal, M.J., Okajima, K., Luk, V.K., 1988, "Penetration of 6061-T651 Aluminum Targets with Rigid Long Rods," Journal of Applied Mechanics, 55:755-760

Hallquist, J.O., 1998, *LS-DYNA Theoretical Manual*, Livermore Software Technology Corporation, Livermore, CA, May, pp. 24.1 - 24.5

Hancock, S.L., 1985, “PISCES 2DELK Theoretical Manual,” PISCES International b.v., Groningenweg 6, 2803 PV Gouda, The Netherlands, August

Jung, J., 2001, *Personal Communication*, December

Mair, H.U., 1999, “Review: Hydrocodes for Structural Response to Underwater Explosions,” *Shock and Vibration*, 6:81-96

Metzinger, K.E. , 1997, “Using PRONTO3D/SPH to Model Penetration Events,” *Internal Memo to N.R.Hansen*, Sandia National Laboratories, Albuquerque, NM, May, 14

Noh, W.F., 1964, “CEL: A Time-Dependent, Two-Space-Dimensional, Coupled Eulerian-Lagrangian Code,” *Methods in Computational Physics, Volume 3, Fundamental Methods in Hydrodynamics*, B.Alder, S.Fernbach, M.Rotenberg, eds., Academic Press, New York, NY, pp. 117-179

Olovsson, L., 2000, “On the Arbitrary Lagrangian-Eulerian Finite Element Method,” *Linköping Studies in Technology, Dissertation No. 635,* Linköpings University, Linköping, Sweden

Panton, R.L., 1984, *Incompressible Flow*, John Wiley and Sons, New York, NY, pp. 554-559

Silling, S.A. 1993, “Simulation of Penetration and Perforation with CTH,” *Advances in Numerical Simulation Techniques for Penetration and Perforation of Solids, AMD-Vol.171*, E.P.Chen, V.K.Luk, ed., American Society of Mechanical Engineers, Applied Mechanics Division, pp. 57-66

Silling, S.A., 2001, “A Meshfree Method Based on the Peridynamic Theory of Solid Mechanics,” *Technical Report SAND2001-2346P*, Sandia National Laboratories, Albuquerque, NM

Swegle, J.W., Attaway, S.W., Heinstein, M.W, Mello, F.J., Hick, D.L. 1993, “An Analysis of Smoothed Particle Hydrodynamics,,” Technical Report SAND93-2513, Sandia National Laboratories, Albuquerque, NM

Vaughan, C.T., Bessette, G.C., Bell, R.L., 2001, *Personal Communication*, November 8

Wingate, C.A., Stellingwerf, R.F., 1993, “Smooth Particle Hydrodynamics: The SPHINX and SPHC Codes,” *Advances in Numerical Simulation Techniques for Penetration and Perforation of Solids, AMD-Vol.171*, E.P.Chen, V.K.Luk, ed., American Society of Mechanical Engineers, Applied Mechanics Division, pp. 75-94

Distribution

1	MS	0318	9230	P.	Yarrington
1	MS	0321	9200	B.	Camp
1	MS	0482	2131	R.	Baty
1	MS	0482	2131	K.	Meeks
1	MS	0482	2131	B.	Mickelsen
1	MS	0482	2131	J.	Wirth
1	MS	0819	9231	E.	Boucheron
5	MS	0819	9231	K.	Brown
1	MS	0819	9231	K.	Budge
5	MS	0819	9231	S.	Burns
1	MS	0819	9231	D.	Caroll
5	MS	0819	9231	M.	Christon
1	MS	0819	9231	A.	Robinson
1	MS	0819	9231	M.	Wong
1	MS	0820	9232	R.	Bell
1	MS	0820	9232	G.	Bessette
1	MS	0820	9232	P.	Chavez
1	MS	0820	9232	S.	Silling
1	MS	0820	9232	R.	Weatherby
1	MS	0835	9140	M.	McGlaun
1	MS	0835	9142	J.	Peery
1	MS	0841	9100	T.	Bickel
1	MS	0847	9126	J.	Jung
1	MS	0847	9126	D.	Longcope
1	MS	1111	9226	C.	Vaughan

1	MS	9018	8945-1	Central Technical Files
2	MS	0899	9616	Technical Library
1	MS	0612	9612	Review and Approval Desk for DOE/OSTI